

# Perdeuterated Conjugated Polymers for Ultralow-Frequency Magnetic Resonance of OLEDs

Sebastian Milster, Tobias Grünbaum, Sebastian Bange, Simon Kurrmann, Hermann Kraus, Dani M. Stoltzfus, Anna E. Leung, Tamim A. Darwish, Paul L. Burn, Christoph Boehme, and John M. Lupton\*

**Abstract:** The formation of excitons in OLEDs is spin dependent and can be controlled by electron-paramagnetic resonance, affecting device resistance and electroluminescence yield. We explore electrically detected magnetic resonance in the regime of very low magnetic fields ( $<1$  mT). A pronounced feature emerges at zero field in addition to the conventional spin- $1/2$  Zeeman resonance for which the Larmor frequency matches that of the incident radiation. By comparing a conventional  $\pi$ -conjugated polymer as the active material to a perdeuterated analogue, we demonstrate the interplay between the zero-field feature and local hyperfine fields. The zero-field peak results from a quasistatic magnetic-field effect of the RF radiation for periods comparable to the carrier-pair lifetime. Zeeman resonances are resolved down to 3.2 MHz, approximately twice the Larmor frequency of an electron in Earth's field. However, since reducing hyperfine fields sharpens the Zeeman peak at the cost of an increased zero-field peak, we suggest that this result may constitute a fundamental low-field limit of magnetic resonance in carrier-pair-based systems. OLEDs offer an alternative solid-state platform to investigate the radical-pair mechanism of magnetic-field effects in photochemical reactions, allowing models of biological magnetoreception to be tested by measuring spin decoherence directly in the time domain by pulsed experiments.

Man kind has mused over the apparent animal compass as far back as the writing of the *Book of Job*,<sup>[1]</sup> although bird migration remained academically controversial until storks impaled by African arrows were found to return to European roosting grounds.<sup>[2]</sup> Different models of biological magnetoreception have been put forward, and for some species, it appears that the photoinduced generation of a radical pair in retinal pigment–protein complexes may hold the key.<sup>[3]</sup> The spins of such a spatially separated radical pair will precess in

hyperfine fields, leading to a departure from the original spin permutation symmetry of the pair. Since most pigments are characterized by singlet ground states, following photoexcitation, singlet states will be formed initially. The charge-separated radical-pair state resulting from electron transfer from the pigment excited state therefore retains singlet character, oscillating in time to the triplet configuration and back again.<sup>[3a]</sup> Because of the spin-singlet symmetry of the ground state, recombination of the radical pair is inhibited in the triplet, and so the overall reaction rates of the radical species are slowed. The net reaction yield therefore depends on the overall singlet content of the pair state—which is modified by an external magnetic field, setting an axis of quantization for the spins and suppressing spin mixing in the hyperfine fields. A crucial test of this radical-pair model of magnetoreception has been the demonstration that birds become disorientated when exposed to radio-frequency (RF) radiation of a frequency close to the Larmor frequency of the electron spin in Earth's field.<sup>[4]</sup> Elegant molecular model systems have been developed to replicate key steps of the photoinduced electron transfer and subsequent spin-dependent recombination in donor–bridge–acceptor triads, both in static magnetic field-effect measurements of reaction yield<sup>[5a]</sup> and in corresponding dynamic resonance experiments.<sup>[5b]</sup> Some triads even exhibit directional sensitivity, i.e., an anisotropy of the magnetic-field effect, due to anisotropic spin–spin coupling.<sup>[6]</sup> Since these experiments are performed in solution, only limited attention has been paid to directly engineering hyperfine field strengths.<sup>[7]</sup>

Spin-dependent recombination of charge carriers is reminiscent of the operating principle of organic light-emitting diodes (OLEDs), where radical anions (electrons) and cations (holes) are injected electrically from opposing electrodes to form molecular excitations of either singlet or triplet spin

[\*] S. Milster, T. Grünbaum, Dr. S. Bange, S. Kurrmann, H. Kraus, Prof. Dr. J. M. Lupton  
Institut für Experimentelle und Angewandte Physik  
Universität Regensburg  
Universitätsstrasse 31, 93053 Regensburg (Germany)  
E-mail: john.lupton@ur.de

Dr. D. M. Stoltzfus, Prof. P. L. Burn  
Centre for Organic Photonics & Electronics, School of Chemistry and Molecular Biosciences, The University of Queensland  
Brisbane, Queensland 4072 (Australia)

Dr. A. E. Leung, Dr. T. A. Darwish  
National Deuteration Facility, Australian Nuclear Science and Technology Organization (ANSTO)  
Locked Bag 2001, Kirrawee DC, NSW 2232 (Australia)

Prof. Dr. C. Boehme  
Department of Physics and Astronomy, University of Utah  
115 South 1400 East, Salt Lake City, UT 84112 (USA)

Supporting information and the ORCID identification number(s) for the author(s) of this article can be found under <https://doi.org/10.1002/anie.202002477>.

© 2020 The Authors. Published by Wiley-VCH Verlag GmbH & Co. KGaA. This is an open access article under the terms of the Creative Commons Attribution Non-Commercial NoDerivs License, which permits use and distribution in any medium, provided the original work is properly cited, the use is non-commercial, and no modifications or adaptations are made.

degeneracy. The yield of these recombinant species is affected by external static and oscillatory magnetic fields.<sup>[8]</sup> Field changes can be detected down to 200 nT, i.e., for fields a hundredfold weaker than Earth's.<sup>[9]</sup> Spin-dependent recombination can be probed through either electroluminescence or resistance change under magnetic resonance,<sup>[10]</sup> the latter being referred to as electrically detected magnetic resonance (EDMR). Most magnetic resonance experiments on OLEDs have focused on the X-band range around 10 GHz and allow coherence times to be measured by spin-echo spectroscopy<sup>[11]</sup> to a level of sensitivity which can even probe nuclear magnetic resonances.<sup>[11c]</sup> Previously, we introduced a stripline design, with which it became possible to resolve resonances at around 100 MHz, a frequency range initially thought to be limited by the local hyperfine-field strengths.<sup>[12]</sup> With careful sampling, however, we recently succeeded in resolving Zeeman resonances down to 5.5 MHz in a commercially available conjugated polymer,<sup>[9b]</sup> a frequency already quite close to the electron's Larmor frequency in geomagnetic fields of  $\approx 0.7$ –1.74 MHz. However, in addition to the anticipated Zeeman resonances, a further feature emerges at low RF frequency:<sup>[9b]</sup> a zero-field peak reminiscent in structure to what has also been reported in reaction-yield detected magnetic resonance (RYDMR).<sup>[13]</sup> Following the results of quantum-dynamical simulations, these features have been attributed to both the RF-induced resonances in the local hyperfine fields as well as to the quasistatic nature of the low-frequency RF magnetic fields experienced by short-lived radical pairs.<sup>[13]</sup> We now explore the nature of the zero-field feature in EDMR by replacing hydrogen atoms in the active layer of the OLED with deuterium.

Figure 1a shows the structure of the perdeuterated version of poly[2-methoxy-5-(2'-ethylhexyloxy)-1,4-phenylenevinylene] (d-MEHPPV).<sup>[14]</sup> Unlike in previous reports of magnetic-field effects in OLEDs,<sup>[15]</sup> this material has the hydrogen atoms of the side chains and polymer backbone replaced by deuterium, rather than merely those associated with the side chains. The effective hyperfine fields,  $B_{\text{hyp}}$ , characterized by the standard deviation of a Gaussian dis-

tribution of hyperfine fields for electron and hole are therefore reduced from 0.72 mT and 0.19 mT for the protonated MEHPPV (h-MEHPPV) to 0.24 mT and 0.08 mT for d-MEHPPV. These values were extracted from a multi-frequency analysis of EDMR spectra.<sup>[14]</sup> Similar values are obtained by analyzing EDMR measurements taken at an excitation frequency of 280 MHz, as detailed in the Supporting Information. This reduction of the EDMR linewidth by a factor of  $\approx 3$  upon deuteration is in line with the hyperfine coupling constant, which is 6.5 times smaller for deuterium than for hydrogen. Since deuterium has a nuclear spin of 1, the inhomogeneous broadening due to the hyperfine fields is expected to decrease by a factor of 3.25 for d-MEHPPV as compared to h-MEHPPV containing hydrogen with a nuclear spin of  $1/2$ . We compare low-field EDMR spectra of OLEDs made of the two polymers. Details of the fabrication process are discussed in the Supporting Information. The OLEDs were placed on a stripline<sup>[8a]</sup> to generate the linearly polarized RF radiation of oscillating magnetic-field amplitude  $B_1$ , and positioned inside three pairs of Helmholtz coils to provide static magnetic fields  $B_0$  of  $\approx 50$  nT precision and arbitrary orientation.<sup>[9b]</sup> Figure 1b shows a sketch of the arrangement. EDMR was detected under forward constant-current bias to give current densities of 1.0–17.5 mA cm<sup>-2</sup>, and recorded with a lock-in amplifier under square-wave RF amplitude modulation at 232 Hz.<sup>[9b]</sup>

Figure 1c compares EDMR spectra of OLEDs composed of the protonated (h) and deuterated (d) polymers at an RF frequency of 8 MHz.<sup>[16]</sup> In addition to the expected Zeeman resonances, a peak is seen at zero field, which is superimposed by the Zeeman resonances at positive and negative fields. The signal near zero field arises in part because of hyperfine fields:<sup>[13]</sup> in the absence of an external field, nuclear magnetic moments result in local effective magnetic fields for the electron and hole spins, taking over the role of the external field  $B_0$  to ensure that some of these are in resonance with the RF field. In addition, however, for short-lived carrier pairs, a slowly oscillating magnetic field  $B_1$  represents a quasistatic contribution to the local magnetic field.<sup>[13b]</sup> The zero-field response is therefore intricately linked to the static magneto-resistance effect as illustrated in Figure S1.

For  $B_1 \parallel B_0$ , the Zeeman resonances should be suppressed for conventional magnetic resonance, providing a possibility to separate the zero-field peak more clearly from the Zeeman resonances. Angle-dependent EDMR measurements are shown in Figure 2. To make the measurements of the two materials comparable, we chose different resonance frequencies to ensure that the zero-field peak and the Zeeman resonances are approximately equally well resolved: 9 MHz for the deuterated compound and 12 MHz for the protonated material. We plot the raw, non-normalized data including the offset introduced by the lock-in detection (this was mitigated in Figure 1<sup>[16]</sup>). For both materials, the Zeeman resonances disappear as  $\alpha$  approaches zero ( $B_1 \parallel B_0$ ), although in contrast to the conventional regime of high  $B_0$  fields they cannot be suppressed completely.<sup>[13b]</sup>

Next, we compare the evolution of EDMR spectra with decreasing RF frequency in Figure 3. The spectra are not normalized but are corrected for the offset introduced by the

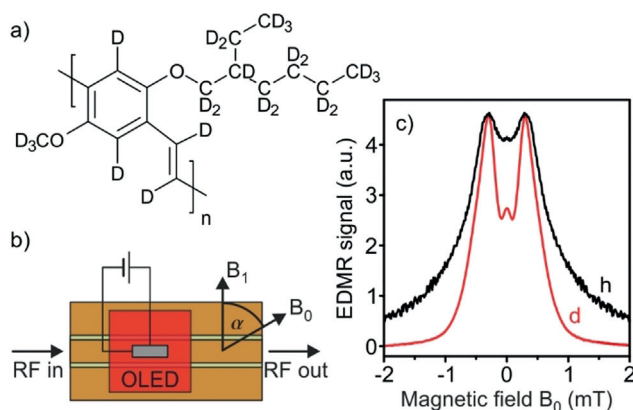


**Figure 1.** Ultralow-field electrically detected magnetic resonance (EDMR) of OLEDs. a) Structure of perdeuterated d-MEHPPV. b) EDMR setup of the OLED placed on an RF stripline with variable in-plane angle  $\alpha$  between the static field  $B_0$  and oscillating field  $B_1$ . c) Comparison of EDMR spectra of h-MEHPPV and d-MEHPPV at 8 MHz.<sup>[16]</sup>

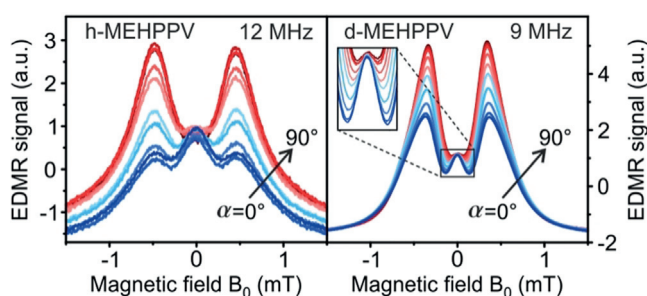


**Figure 2.** Dependence of EDMR spectra on angle  $\alpha$ . With the Zeeman resonance suppressed for  $B_0 \parallel B_1$ , the zero-field peak is resolved. Measurements were performed at 5 W RF power and  $17.5 \text{ mA cm}^{-2}$  device current density.

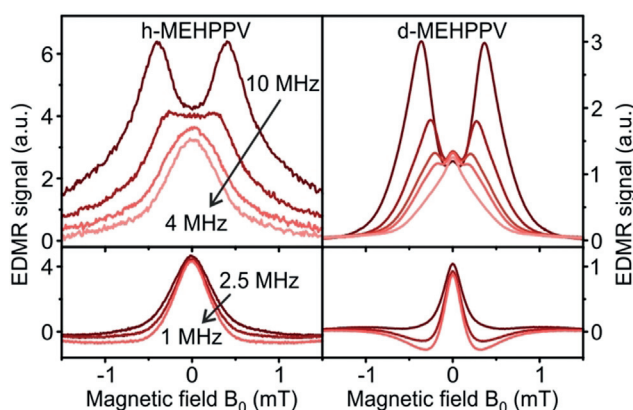


**Figure 3.** Frequency dependence of EDMR line shape for  $\alpha = 90^\circ$ . The Zeeman resonances disappear with decreasing frequency, revealing the zero-field peak. At frequencies below 2.5 MHz, partial inversion of the signal occurs. Measurements were performed at 8 W RF power and a current density of  $3.5 \text{ mA cm}^{-2}$ . The RF frequencies are 4.0, 5.0, 5.5 (deuterated only), 7.0, and 10 MHz (upper panel); and 1.0, 1.5, 2.5 MHz (lower panel).

lock-in amplifier as described in the Supporting Information. We separate the data into frequencies above 4 MHz (upper panels) and below. In the low-frequency regime, the amplitude of the zero-field feature does not change with frequency. For the protonated compound, Zeeman resonances are resolved down to 7 MHz, below which they become inseparable from the zero-field peak. This transition occurs at 3.2 MHz for the deuterated material. Detailed spectra from the transition region are shown in the Supporting Information. Below 2.5 MHz, a partial inversion of the signal develops, which is more pronounced for the deuterated polymer. This unusual spectral shape and change of amplitude sign at low frequencies is reminiscent of RYDMR spectra.<sup>[7b,13]</sup> We speculate that this transition in spectral shape may be linked to the OLED response to  $B_1$  becoming effectively quasistatic as the period of the RF radiation exceeds the carrier-pair lifetime of order  $1 \mu\text{s}$ .<sup>[17]</sup> In this case, the RF radiation modulates the magnetoresistance rather than inducing a true magnetic resonance. Since the curvature of the magnetoresistance of d-MEHPPV is much larger than for h-MEHPPV<sup>[14]</sup> (see Figure S1), the zero-field peak and the inversion of the signal at finite  $B_0$  are more pronounced for

the deuterated polymer. This effect is likely linked to an increase of the zero-field peak with increasing device current (not shown), which presumably lowers the carrier-pair lifetime.

Finally, we examine the effect of RF power on the zero-field feature. From the power broadening<sup>[18a]</sup> and the RF current flowing through the stripline,<sup>[18b]</sup> we estimate the maximal amplitude of  $B_1$  to be of order  $100 \mu\text{T}$ . The spectra, plotted in Figure 4, show a substantial influence of RF power.

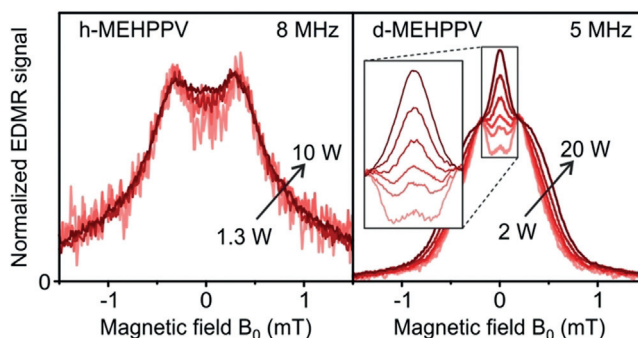


**Figure 4.** Power dependence of the zero-field EDMR feature. With increasing RF power (1.3, 2.5, 5.0, 10 W for h-MEHPPV at 8 MHz; and 2.0, 4.0, 5.0, 8.0, 12.6, 20 W for d-MEHPPV at 5 MHz), the zero-field peak rises.<sup>[16]</sup>

Surprisingly, the power dependence is much stronger for the perdeuterated compound than for the protonated material. Raising the amplitude of  $B_1$  increases the range of effective quasistatic magnetic fields probed by the magnetoresistive response of the OLED, and thus promotes the zero-field signal. The weaker the hyperfine fields, the stronger the variation in the magnetoresistance response for small changes of the total magnetic field. The strong dependence of the zero-field feature on  $B_1$  amplitude for the perdeuterated compound is thus in agreement with the steep magnetoresistance response of this material in the field range of a few hundred microtesla, shown in Figure S1a. Concurrently, power-broadening effects of the Zeeman resonances are more pronounced for the perdeuterated than for the protonated material, where hyperfine field-induced inhomogeneous broadening is greater. The zero-field features do not appear to be affected by power broadening, consistent with the interpretation that they are not primarily due to a paramagnetic resonance.

While OLEDs offer a method of exploring the hyperfine field-induced spin-mixing processes invoked in the radical-pair mechanism of magnetoreception,<sup>[19]</sup> even removing 95% of the hydrogen nuclei<sup>[14]</sup> in the perdeuterated MEHPPV used here does not allow us to conclusively resolve Zeeman resonances at geomagnetic field strengths. Suitable molecular candidate complexes for the radical-pair mechanism in biological systems, free of any hydrogen isotopes, have been identified—at least for one of the two spins.<sup>[19]</sup> Since hydrogen is ubiquitous in organic electronics, we propose developing larger polycyclic aromatic hydrocarbons for OLEDs, where the spins become localized sufficiently far away from the

hydrogenic nuclei. In such graphene fragments, however, spin-orbit coupling<sup>[18b]</sup> may be stronger and can give rise to additional dephasing obscuring ultralow-field resonances. It is also conceivable that carrier-pair lifetimes, which limit coherence,<sup>[11a]</sup> can be raised in blend materials. Since spin decoherence can be measured directly in OLEDs,<sup>[11]</sup> we aim to devise RF pulse sequences to reverse dephasing and probe decoherence at ultralow fields. Under these conditions,  $B_1$  and  $B_0$  are of comparable magnitude and coherence is predicted to become protected by formation of the collective spin-Dicke state.<sup>[20]</sup> In this context, it is interesting to note the similarity of hyperfine-driven coherent singlet-triplet mixing of spin pairs in OLEDs to the formation of entangled carrier-pair species in spin-qubit coupled quantum dots.<sup>[21]</sup> Given our observation that a reduction in hyperfine coupling sharpens the Zeeman resonance while raising the zero-field peak because of the quasistatic  $B_1$  contributions, we conclude that there may be a fundamental lower field limit to resolving Zeeman resonances.

A somewhat poorly defined parameter of the radical-pair model is the lifetime of the carrier pair; presumably, a distribution of lifetimes exists, since there is a range of possible molecular conformations. For a resonance to occur, the carrier-pair lifetime must exceed the inverse Larmor frequency. We stress the importance of differentiating between resonant and quasistatic contributions to EDMR, that is, magnetic-field effects which occur on timescales significantly shorter or longer than the pair lifetime, respectively. A distinction between these processes is likely also relevant to behavioural studies involving exposure of birds to RF radiation in the exploration of mechanisms of the avian compass.<sup>[4]</sup> Microscopic modelling of the transition from resonant to non-resonant field effects may offer an avenue to extract the carrier-pair lifetime distribution. Finally, we speculate that such a differentiation between resonant and non-resonant spin-dependent phenomena could be quite generic to the radical-pair mechanism itself. Low-field effects appear to be primarily static in nature, but it is conceivable that molecular dynamics could give rise to an effective broadband oscillatory component of the hyperfine field—an effective isotropic  $B_1$  spanning a broad frequency range. On this premise, the molecular dynamics could lead to a resonance of long-lived pairs at very low  $B_0$ , with non-trivial collective, i.e. spin-Dicke-type, resonant transitions emerging when Rabi and Larmor frequency become comparable.<sup>[20,22]</sup> This condition of light-matter interaction is referred to as the “ultrastrong drive” regime,<sup>[18]</sup> transitions not only become quantum-mechanically reversible, but spin states form coherent superpositions with the “photon” states of the resonant radiation. Identification of such “intrinsic” resonance phenomena in ultra-small magnetic-field effects in the absence of external RF radiation will necessitate sophisticated microscopic quantum-dynamical modelling of the highly non-perturbative interaction between spins and oscillating magnetic fields. Perhaps there is more to magnetoreception than meets the eye?

## Acknowledgements

Funded by the Deutsche Forschungsgemeinschaft (DFG, German Research Foundation) – Project-ID 314695032 – SFB 1277. P.L.B. is an Australian Research Council Laureate Fellow (FL160100067). The National Deuterium Facility is partly funded by NCRIS, an Australian Government initiative.

## Conflict of interest

The authors declare no conflict of interest.

**Keywords:** conjugated polymers · deuteration · isotopes · magnetic resonance · organic light-emitting diodes

- [1] Book of Job 39:26.
- [2] H. Schildmacher, *Der Falke* **1972**, *19*, 222–227.
- [3] a) T. Ritz, S. Adem, K. Schulten, *Biophys. J.* **2000**, *78*, 707–718; b) C. T. Rodgers, P. J. Hore, *Proc. Natl. Acad. Sci. USA* **2009**, *106*, 353–360.
- [4] a) T. Ritz, P. Thalau, J. B. Phillips, R. Wiltschko, W. Wiltschko, *Nature* **2004**, *429*, 177–180; b) S. Engels, N.-L. Schneider, N. Lefeldt, C. M. Hein, M. Zapka, A. Michalik, D. Elbers, A. Kittel, P. J. Hore, H. Mouritsen, *Nature* **2014**, *509*, 353–356.
- [5] a) K. Maeda, K. B. Henbest, F. Cintolesi, I. Kuprov, C. T. Rodgers, P. A. Liddell, D. Gust, C. R. Timmel, P. J. Hore, *Nature* **2008**, *453*, 387–390; b) K. Maeda, J. G. Storey, P. A. Liddell, D. Gust, P. J. Hore, C. J. Wedge, C. R. Timmel, *Phys. Chem. Chem. Phys.* **2015**, *17*, 3550–3559.
- [6] C. Kerpel, S. Richert, J. G. Storey, S. Pillai, P. A. Liddell, D. Gust, S. R. Mackenzie, P. J. Hore, C. R. Timmel, *Nat. Commun.* **2019**, *10*, 3707.
- [7] a) J. R. Woodward, C. R. Timmel, K. A. McLauchlan, P. J. Hore, *Phys. Rev. Lett.* **2001**, *87*, 077602; b) C. J. Wedge, C. T. Rodgers, S. A. Norman, N. Baker, K. Maeda, K. B. Henbest, C. R. Timmel, P. J. Hore, *Phys. Chem. Chem. Phys.* **2009**, *11*, 6573–6579.
- [8] a) H. Kraus, S. Bange, F. Frunder, U. Scherf, C. Boehme, J. M. Lupton, *Phys. Rev. B* **2017**, *95*, 241201; b) A. J. Schellekens, W. Wagemans, S. P. Kersten, P. A. Bobbert, B. Koopmans, *Phys. Rev. B* **2011**, *84*, 075204; c) Y. Yoshida, A. Fujii, M. Ozaki, K. Yoshino, E. Frankevich, *Mol. Cryst. Liq. Cryst.* **2005**, *426*, 19–24.
- [9] a) P. Klemm, S. Bange, A. Pöllmann, C. Boehme, J. M. Lupton, *Phys. Rev. B* **2017**, *95*, 241407; b) T. Grünbaum, S. Milster, H. Kraus, W. Ratzke, S. Kurrmann, V. Zeller, S. Bange, C. Boehme, J. M. Lupton, *Faraday Discuss.* **2020**, *221*, 92–109.
- [10] L. S. Swanson, J. Shinar, A. R. Brown, D. D. C. Bradley, R. H. Friend, P. L. Burn, A. Kraft, A. B. Holmes, *Phys. Rev. B* **1992**, *46*, 15072–15077.
- [11] a) W. J. Baker, T. L. Keevers, J. M. Lupton, D. R. McCamey, C. Boehme, *Phys. Rev. Lett.* **2012**, *108*, 267601; b) A. J. Kupijai, K. M. Behringer, F. G. Schaeble, N. E. Galfé, M. Corazza, S. A. Gevorgyan, F. C. Krebs, M. Stutzmann, M. S. Brandt, *Phys. Rev. B* **2015**, *92*, 245203; c) H. Malissa, M. Kavand, D. P. Waters, K. J. van Schooten, P. L. Burn, Z. V. Vardeny, B. Saam, J. M. Lupton, C. Boehme, *Science* **2014**, *345*, 1487–1490.
- [12] W. J. Baker, K. Ambal, D. P. Waters, R. Baarda, H. Morishita, K. van Schooten, D. R. McCamey, J. M. Lupton, C. Boehme, *Nat. Commun.* **2012**, *3*, 898.
- [13] a) C. T. Rodgers, C. J. Wedge, S. A. Norman, P. Kukura, K. Nelson, N. Baker, K. Maeda, K. B. Henbest, P. J. Hore, C. R.

- Timmel, *Phys. Chem. Chem. Phys.* **2009**, *11*, 6569–6572; b) C. R. Timmel, P. J. Hore, *Chem. Phys. Lett.* **1996**, *257*, 401–408.
- [14] D. M. Stoltzfus, G. Joshi, H. Popli, S. Jamali, M. Kavand, S. Milster, T. Grünbaum, S. Bange, A. Nahlawi, M. Y. Teferi, S. I. Atwood, A. E. Leung, T. A. Darwish, H. Malissa, P. L. Burn, J. M. Lupton, C. Boehme, *J. Mater. Chem. C* **2020**, *8*, 2764–2771.
- [15] a) S.-Y. Lee, S.-Y. Paik, D. R. McCamey, J. Yu, P. L. Burn, J. M. Lupton, C. Boehme, *J. Am. Chem. Soc.* **2011**, *133*, 2019–2021; b) T. D. Nguyen, G. Hukic-Markosian, F. Wang, L. Wojcik, X.-G. Li, E. Ehrenfreund, Z. V. Vardeny, *Nat. Mater.* **2010**, *9*, 345–352; c) J. E. Lawrence, A. M. Lewis, D. E. Manolopoulos, P. J. Hore, *J. Chem. Phys.* **2016**, *144*, 214109.
- [16] To make the spectra comparable, they are corrected for the offset introduced by the lock-in amplifier and normalized. Details of this procedure are given in the Supporting Information.
- [17] D. R. McCamey, S. Y. Lee, S.-Y. Paik, J. M. Lupton, C. Boehme, *Phys. Rev. B* **2010**, *82*, 125206.
- [18] a) S. Jamali, G. Joshi, H. Malissa, J. M. Lupton, C. Boehme, *Nano Lett.* **2017**, *17*, 4648–4653; b) G. Joshi, R. Miller, L. Ogden, M. Kavand, S. Jamali, K. Ambal, S. Venkatesh, D. Schurig, H. Malissa, J. M. Lupton, C. Boehme, *Appl. Phys. Lett.* **2016**, *109*, 103303.
- [19] P. J. Hore, H. Mouritsen, *Annu. Rev. Biophys.* **2016**, *45*, 299–344.
- [20] R. C. Roundy, M. E. Raikh, *Phys. Rev. B* **2013**, *88*, 125206.
- [21] a) F. H. L. Koppens, J. A. Folk, J. M. Elzerman, R. Hanson, L. H. Willems van Beveren, I. T. Vink, H. P. Tranitz, W. Wegscheider, L. P. Kouwenhoven, L. M. K. Vandersypen, *Science* **2005**, *309*, 1346–1350; b) B. M. Maune, M. G. Borselli, B. Huang, T. D. Ladd, P. W. Deelman, K. S. Holabird, A. A. Kiselev, I. Alvarado-Rodriguez, R. S. Ross, A. E. Schmitz, M. Sokolich, C. A. Watson, M. F. Gyure, A. T. Hunter, *Nature* **2012**, *481*, 344–347; c) J. R. Petta, A. C. Johnson, J. M. Taylor, E. A. Laird, A. Yacoby, M. D. Lukin, C. M. Marcus, M. P. Hanson, A. C. Gossard, *Science* **2005**, *309*, 2180–2184.
- [22] D. P. Waters, G. Joshi, M. Kavand, M. E. Limes, H. Malissa, P. L. Burn, J. M. Lupton, C. Boehme, *Nat. Phys.* **2015**, *11*, 910–914.

Manuscript received: February 17, 2020

Accepted manuscript online: March 13, 2020

Version of record online: April 6, 2020